

Provided for non-commercial research and education use.
Not for reproduction, distribution or commercial use.



This article appeared in a journal published by Elsevier. The attached copy is furnished to the author for internal non-commercial research and education use, including for instruction at the authors institution and sharing with colleagues.

Other uses, including reproduction and distribution, or selling or licensing copies, or posting to personal, institutional or third party websites are prohibited.

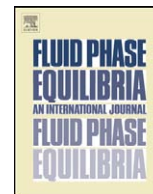
In most cases authors are permitted to post their version of the article (e.g. in Word or Tex form) to their personal website or institutional repository. Authors requiring further information regarding Elsevier's archiving and manuscript policies are encouraged to visit:

<http://www.elsevier.com/copyright>



Contents lists available at ScienceDirect

Fluid Phase Equilibria

journal homepage: www.elsevier.com/locate/fluid

A comparative study of particle swarm optimization and its variants for phase stability and equilibrium calculations in multicomponent reactive and non-reactive systems

Adrián Bonilla-Petriciolet^{a,*}, Juan Gabriel Segovia-Hernández^b^a Instituto Tecnológico de Aguascalientes, Chemical Engineering Department, C.P. 20256 Aguascalientes, Mexico^b Universidad de Guanajuato, Chemical Engineering Department, Campus Guanajuato, C.P. 36050 Guanajuato, Mexico

ARTICLE INFO

Article history:

Received 10 August 2009

Received in revised form 2 November 2009

Accepted 5 November 2009

Available online 11 November 2009

Keywords:

Phase stability

Phase equilibrium

Particle swarm optimization

Chemical equilibrium

ABSTRACT

Particle swarm optimization is a novel evolutionary stochastic global optimization method that has gained popularity in the chemical engineering community. This optimization strategy has been successfully used for several applications including thermodynamic calculations. To the best of our knowledge, the performance of PSO in phase stability and equilibrium calculations for both multicomponent reactive and non-reactive mixtures has not yet been reported. This study introduces the application of particle swarm optimization and several of its variants for solving phase stability and equilibrium problems in multicomponent systems with or without chemical equilibrium. The reliability and efficiency of a number of particle swarm optimization algorithms are tested and compared using multicomponent systems with vapor–liquid and liquid–liquid equilibrium. Our results indicate that the classical particle swarm optimization with constant cognitive and social parameters is a reliable method and offers the best performance for global minimization of the tangent plane distance function and the Gibbs energy function in both reactive and non-reactive systems.

© 2009 Elsevier B.V. All rights reserved.

1. Introduction

Phase equilibrium calculations play a major role in the design, development, operation, optimization and control of chemical processes. These calculations involve both phase stability analysis and split computations with or without the presence of chemical reactions. For a given mixture with specified composition, temperature and pressure, the phase stability analysis is used to check if the tested phase is stable or not. If it is not stable then the phase split calculations can be performed, and the stability status of the new phases (obtained from split calculation) is again tested. The modeling of phase behavior of multicomponent reactive and non-reactive systems is a complex topic due to non-linear interactions among components, phases and reactions. Therefore, the development of reliable methods for solving phase equilibrium problems has long been a challenge and remains so [1].

Phase equilibrium calculations can be formulated as a global optimization problem where the tangent plane distance function (*TPDF*) is used as optimization criterion for stability analysis

and the Gibbs energy function (*G*) is minimized for phase split computations [1–4]. Specifically, global optimization problems for phase and stability calculations in reactive and non-reactive systems follow the form: minimize $f(u)$ subject to $u \in \Omega$ where u is a continuous variable vector with domain $\Omega \in \mathbb{R}^n$, and $f(u): \Omega \rightarrow \mathbb{R}$ is a real-valued function. The domain Ω is defined within upper and lower limits of each decision variable, which are generally mole numbers or mole fractions for phase equilibrium calculations. The minimization of *G* and *TPDF* (i.e., $f(u)$) can be performed using both equation-solving methods and direct optimization strategies [5–7]. If chemical reactions occur in the mixture, these strategies can also be classified as either stoichiometric or non-stoichiometric, depending on the formulation of material balance constraints [8]. Equation-solving methods are based on the solution of non-linear equations obtained from the stationary conditions of the optimization criterion. Local search methods with and without decoupling strategies are frequently used to solve these equations in conjunction with mass balance restrictions. However, these methods are prone to severe computational difficulties and may fail to converge when initial estimates are not suitable, especially for strongly non-ideal multicomponent and multireactive systems [5–7]. It is worth noting that the mathematical properties of the objective functions used for phase equilibrium calculations depend completely on the structure of the thermodynamic equation chosen to model each of the phases that may exist at equilibrium. Thus, *TPDF* and *G* are

* Corresponding author at: Instituto Tecnológico de Aguascalientes, Ing. Química, Av. López Mateos 1801, 20256 Aguascalientes, Aguascalientes, Mexico. Tel.: +52 449 910 5002; fax: +52 449 910 5002x127.

E-mail address: petriciolet@hotmail.com (A. Bonilla-Petriciolet).

generally non-convex, highly non-linear with many decision variables, and often have unfavorable attributes such as discontinuity and non-differentiability (e.g. when cubic equations of state or asymmetric models are used for modeling thermodynamic properties). As a consequence, they may have several local minimums including trivial and nonphysical solutions. In these conditions, conventional numerical methods are not suitable for solving phase equilibrium problems in both reactive and non-reactive systems.

Minimization strategies are preferred by researchers in process modeling to study mixtures with complex phase behavior. Most of the available methods for minimization of *TPDF* and *G* have been proposed during recent decades, and they comprise local and global optimization approaches [5–7]. Reviews of several studies using minimization strategies for phase equilibrium calculations can be found in Teh and Rangaiah [5] and Wakeman and Staveva [7] for non-reactive systems, and in Seider and Widagdo [6] for reactive mixtures. In general, these reviews indicate that there has been a significant and increasing interest in the development of deterministic and stochastic global strategies for reliably solving phase equilibrium problems. Studies on deterministic phase equilibrium calculations have been focused on the application of homotopy continuation methods [9–13], branch and bound global optimization [14–16] and interval analysis using an interval-Newton/generalized bisection algorithm [17–19]. Although these methods have proven to be very promising, several of them are model dependent, may require problem reformulations or significant computational time for multicomponent systems [7,20].

Alternatively, stochastic optimization techniques have often been found to be as reliable and effective as deterministic methods but may offer more advantages for phase equilibrium calculations [21]. These methods are robust numerical tools that present a reasonable computational effort in the optimization of multivariable functions (generally less time than deterministic approaches); they are applicable to ill-structure or unknown structure problems, require only calculations of the objective function and can be used with all thermodynamic models. Many thermodynamic problems that are very difficult to solve by conventional techniques can be solved by stochastic methods. To date, several stochastic global optimization methods have been studied and tested for phase equilibrium calculation in non-reactive and reactive mixtures. These methods include: the random search method of Lee et al. [22], simulated annealing [23–26], genetic algorithms [24,27], tabu search [28–30], tunneling method [1,20,31], clustering method with stochastic sampling [21], and differential evolution [29,30,32]. On the other hand, few attempts have been made in the application of stochastic methods for reactive phase equilibrium calculations, compared to those reported for non-reactive systems [22,25,26,30]. The presence of chemical equilibrium constraints increases the complexity and dimensionality of phase equilibrium problems and, as expected, these calculations are more challenging.

One of the most-promising stochastic methods is particle swarm optimization (PSO) [33–43]. This is a novel evolutionary algorithm capable of handling the difficult characteristics of global optimization problems with several decision variables. PSO is simpler, both in formulation and computer implementation, than other population-based metaheuristics. This optimization method has a flexible and well-balanced mechanism to enhance global and local exploration abilities. PSO has become a popular optimization strategy for the chemical engineering community and has been successfully applied in non-linear parameter estimation [36], process design [37,38], and thermodynamic calculations [39–43]. In the literature, there are few studies concerning the application of PSO for phase equilibrium calculations in binary and ternary non-reactive systems [40–42]. Specifically, Cheng et al. [40] reported a linear constraint PSO algorithm for the minimization of *TPDF*. In another study, Cheng and Chen [41] applied a hybrid PSO for Gibbs

energy minimization in ternary systems. Recently, Rahman et al. [42] introduced the application of repulsive particle swarm optimization, another variant of PSO, for solving both phase equilibrium and stability problems in binary and ternary non-reactive mixtures. Unfortunately, the potential of PSO has not been demonstrated by applying it to multicomponent systems, taking into account the fact that problems with higher dimensions are expected to be more difficult to solve than those with lower dimensions, because multicomponent systems can exhibit a variety of possible phase equilibria. Moreover, the capabilities of PSO and its variants have not yet been studied in the modeling of phase behavior for reactive systems even though preliminary results indicate that PSO may offer competitive performance for these calculations [43].

In this study, the feasibility of applying PSO-based algorithms to phase stability and equilibrium calculations in multicomponent reactive and non-reactive systems is studied. Specifically, we test and compare the performance of PSO and several of its variants using phase stability and equilibrium problems with dimension ranging from 2 to 10. This algorithm comparison is necessary to identify the relative strengths of PSO and to justify the choice of a specific algorithm. To the best of our knowledge, this comparative study has not been thoroughly done before. Our results show that the classical particle swarm optimization is a suitable alternative numerical tool for modeling phase behavior of reactive and non-reactive systems.

2. Particle swarm optimization and its variants

Particle swarm optimization is a novel and promising population-based method that belongs to the class of swarm intelligence algorithms. Kennedy and Eberhart [33] introduced this strategy for global optimization, inspired by the social behavior of flocking swarms of birds and fish schools. It exploits a population of potential solutions to identify promising areas for optimization. In this context, the population of potential solutions is called the *swarm* and each solution is called a *particle*. *Particles* are conceptual entities, which fly through the multi-dimensional search space. The success histories of the particles influence both their own search patterns and those of their peers. Each particle has two state variables: its current position $s_{i,j}(k)$ and its current velocity $V_{i,j}(k)$ where k is an iteration counter. In the local version of PSO, which is used in this study, the search is focused on promising regions by biasing each particle's velocity towards both the particle's own remembered best position ($s_{i,j}^p$) and the communicated best ever neighborhood location ($s_{i,j}^{best}$). The relative weights of these two positions are scaled by the cognitive (c_1) and social (c_2) parameters. The cognitive parameter has a contribution towards the self-exploration (or experience) of a particle, while the social parameter has a contribution towards motion of the particles in the global direction taking into account the swarm motion in the preceding iteration. So, the position and velocity of the swarm are updated using:

$$s_{i,j}(k+1) = s_{i,j}(k) + V_{i,j}(k+1) \quad \text{for } i = 1, \dots, n_{var}, \quad j = 1, \dots, n_p \quad (1)$$

$$V_{i,j}(k+1) = c_1 R_1 (s_{i,j}^p - s_{i,j}(k)) + c_2 R_2 (s_{i,j}^{best} - s_{i,j}(k)) \quad \text{for } i = 1, \dots, n_{var}, \quad j = 1, \dots, n_p \quad (2)$$

where $R_1, R_2 \in (0, 1)$ are random numbers, n_{var} is the number of decision variables and n_p is the swarm size (i.e. overall number of particles). Usually, the velocity of each particle is restricted to a maximum value within the interval $[-V^{max}, V^{max}]$, which is defined considering the bounds on decision variables. The lim-

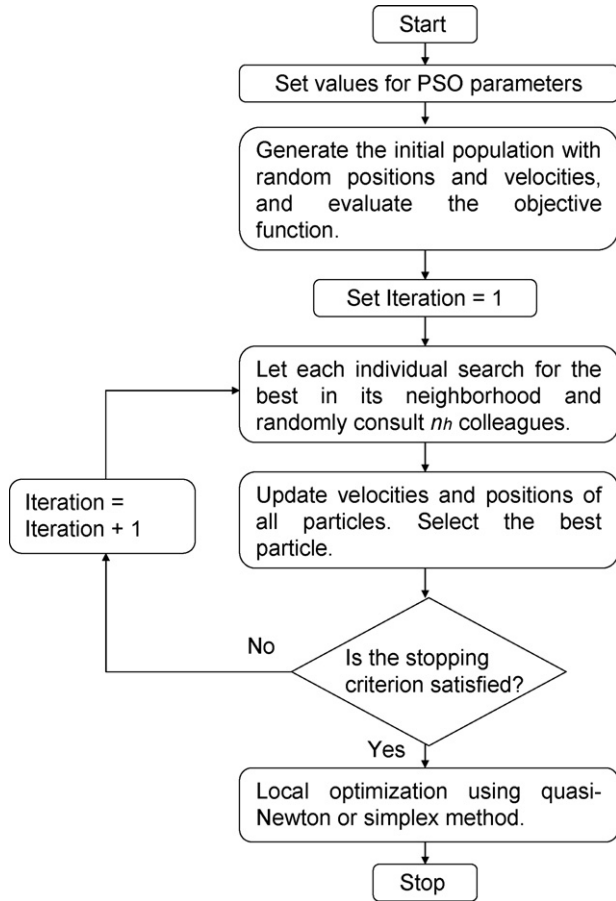


Fig. 1. Flowchart of particle swarm optimization.

itation of maximum velocity of each particle is used to reduce excessively large step sizes in the position rule. In PSO, each particle is assigned to a neighborhood of a pre-specified size. Thus, the best position ever attained by n_h particles that comprise the neighborhood is communicated among them. We have used a random Ring topology for neighborhood communication. After calculating the velocities and position for the next iteration $k + 1$, the current iteration is completed. The best particle is only updated when a new one is found yielding a decrease in the objective function value. These steps are performed until satisfaction of the specified stopping criterion. In this study, this standard version of PSO is referred to as PSO-C. Fig. 1 provides the corresponding flowchart for PSO.

In the literature, many modifications have been proposed to improve the convergence performance of the original PSO [34,35,44,45]. These modifications are generally based on introducing new algorithm parameters (e.g. constriction factor or inertia weight) to modify the velocity rule. Other studies have examined the hybridization of PSO with both local and global search strategies [35]. Below, typical PSO variants are described.

In the original version of PSO, Kennedy and Eberhart [33] suggested that the cognitive and social scaling parameters are fixed constant and equal to $c_1 = c_2 = 2.0$ in order to allow a mean of 1 when multiplied by the random numbers. However, previous numerical experience indicates that it is advantageous to adjust the cognitive/social ratio to favor cognitive learning. In particular, the dynamic values of these parameters may improve the global search over the entire search space during the early iterations and encourage the particles to converge to global optimum at the end of the optimization sequence [34]. Therefore, we have considered a PSO

with dynamic c_1 and c_2 (referred to as PSO-D) where c_1 decreases linearly from $c_{1,0}$ to 0.5 using:

$$c_1 = (0.5 - c_{1,0}) \left(\frac{k}{Iter_{max}} \right) + c_{1,0} \quad (3)$$

where $c_{1,0}$ is the initial value for cognitive parameter, k is the iteration counter and $Iter_{max}$ is the maximum number of iterations allowed for PSO. Note that $c_2 = l - c_1$ where l is defined by the user and is usually ≥ 4 [34].

Recently, Shi and Eberhart [44] proposed a significant variation on the original PSO by introducing the inertia term w into the original velocity rule. The inertia weight factor is used to control the impact of the previous velocities on the current velocity. It also influences the trade-off between the global and local exploration abilities of the particles. The velocity is updated using w as follows:

$$V_{i,j}(k+1) = wV_{i,j}(k) + c_1R_1(s_{i,j}^p - s_{i,j}(k)) + c_2R_2(s_{i,j}^{best} - s_{i,j}(k)) \quad (4)$$

for $i = 1, \dots, n_{var}, j = 1, \dots, n_p$

The literature indicates that high values for inertia term result in straight particle trajectories with significant overshooting at the target, while lower values result in erratic particle trajectories with a reduction of overshoot, both desirable properties for a refined localized search [34]. Typically, an intermediate value of w is selected. This version of PSO is referred to as PSO-I.

Alternatively, a linear inertia reduction is a suitable modification to improve the performance of PSO because, at the initial stage of the search process, large inertia weight is recommended to enhance global exploration; meanwhile, at its last stage, this parameter can be reduced for better local exploration. This algorithm modification attempts to eliminate several of the drawbacks of constant inertia and entails linear scaling of the inertia parameter during the search. Usually, this linear reduction performs between 0.8 and 0.4 in a specified number of function evaluations or iterations. This promotes the gradual shift of PSO from an algorithm suitable for global search to an algorithm suitable for refining an optimum in a local search [34,35]. In this version of PSO (PSO-DI), w decreases linearly from w_0 to 0.4 over the entire run by using:

$$w = (0.4 - w_0) \left(\frac{k}{Iter_{max}} \right) + w_0 \quad (5)$$

In PSO-DI, the swarm velocity is updated using Eqs. (4) and (5).

In a recent study, Clerc and Kennedy [45] introduced constriction factor (κ) into the velocity rule. This parameter also has the effect of reducing particle velocity as the search progresses, thereby contracting the overall swarm diameter and resulting in a progressively smaller search area. Constriction factor is obtained from c_1 and c_2 as follows:

$$\kappa = \frac{2}{|2 - l - \sqrt{l^2 - 4l}|} \quad (6)$$

where $l = c_1 + c_2$ and $l > 4$. Then, the swarm velocity is updated using:

$$V_{i,j}(k+1) = \kappa(V_{i,j}(k) + c_1R_1(s_{i,j}^p - s_{i,j}(k)) + c_2R_2(s_{i,j}^{best} - s_{i,j}(k))) \quad (7)$$

for $i = 1, \dots, n_{var}, j = 1, \dots, n_p$

Results have shown that incorporation of constriction factor into PSO can search different regions efficiently by avoiding premature convergence, and generates higher quality solutions [45]. This PSO variation is referred to as PSO-CF. The characteristics of PSO variants used in this study are given in Table 1 and we have implemented the methods in FORTRAN subroutines.

Finally, the choice of stopping criterion can significantly influence the reliability and efficiency of stochastic optimization

Table 1

Characteristics of PSO variants used for phase stability and equilibrium calculations in reactive and non-reactive systems.

Acronym	Remarks
PSO-C	Particle swarm optimization with constant c_1 and c_2 . Swarm position and velocity are given by Eqs. (1) and (2).
PSO-D	Particle swarm optimization with dynamic c_1 and c_2 (Eq. (3)). Swarm position and velocity are given by Eqs. (1) and (2).
PSO-I	Particle swarm optimization with constant inertia weight w and constant c_1 and c_2 . Swarm position and velocity are given by Eqs. (1) and (4).
PSO-DI	Particle swarm optimization with dynamic inertia weight w (Eq. (5)) and constant c_1 and c_2 . Swarm position and velocity are given by Eqs. (1) and (4).
PSO-CF	Particle swarm optimization with constant c_1 and c_2 and constriction factor. Swarm position and velocity are given by Eqs. (1), (6) and (7).

methods including PSO [1]. In the literature, mainly two stopping criteria are applied for global optimization using stochastic methods [1,28,29,32]: (a) a maximum number of iterations ($Iter_{max}$) and (b) a maximum number of successive iterations (Sc_{max}) without improvement in the best function value. Thus, these criteria are used in this study for the assessment of PSO-based algorithms.

3. Formulation of phase stability and equilibrium problems in non-reactive and reactive mixtures

3.1. Phase stability

Stability analysis is a fundamental stage in phase equilibrium calculations and allows identification of the thermodynamic state that corresponds to the global minimum of Gibbs free energy. A mixture at a fixed temperature T , pressure P and overall composition is stable if and only if the Gibbs free energy surface is at no point below the tangent plane to the surface at the given mixture composition [3,4]. This statement is a necessary and sufficient condition for global stability. Stability analysis can be performed using the tangent plane distance function (*TPDF*). Specifically, phase stability of a non-reactive mixture with c components and a global composition $z(z_1, \dots, z_c)$ in mole fraction units, at constant P and T , is analyzed by the global minimization of *TPDF* [3,4]:

$$TPDF = \sum_{i=1}^c y_i (\mu_{i|y} - \mu_{i|z}) \quad (8)$$

where $\mu_{i|y}$ and $\mu_{i|z}$ are the chemical potentials of component i calculated at compositions y and z , respectively. *TPDF* is the distance between the Gibbs free energy surface at y and the tangent plane constructed to this surface at z [4]. To perform a stability analysis, *TPDF* must be globally minimized with respect to composition of a trial phase y . If the global minimum of *TPDF* < 0 , the mixture under analysis is considered unstable; otherwise it is a globally stable system.

For reactive systems, the stability criterion can be employed in exactly the same way as in phase equilibrium calculations under non-reactive conditions, but for mixtures that are both physically and chemically equilibrated [4,8,13,19]. However, Wasylkiewicz and Ung [12] have proposed an extension of *TPDF* in terms of the reaction-invariant composition variables of Ung and Doherty [46,47]. This alternative stability criterion retains all characteristics and advantages of the classical *TPDF* equation, including a significant reduction in problem dimensionality, and it appears to be more suitable for the modeling of multireactive mixtures [12].

In particular, Ung and Doherty [46,47] proposed the reaction-invariant composition variables for modeling the phase behavior of reactive systems. These variables depend only on the initial com-

position of each independent chemical species. They also restrict the solution space to the compositions that satisfy stoichiometry requirements and reduce the dimension of the composition space by the number of independent reactions. These features allow all of the procedures used to obtain thermodynamic properties of non-reactive mixtures to be extended to systems subject to chemical equilibrium, and, consequently, non-reactive phase equilibrium algorithms can be easily modified to account for chemical reactions [46,47]. In this study, this thermodynamic framework has been used in the formulation of phase stability and equilibrium problems for systems subject to chemical equilibrium.

For a system of c components that undergoes r independent chemical reactions, the transformed mole fractions X_i are defined selecting r reference components:

$$X_i = \frac{x_i - v_i N^{-1} x_{ref}}{1 - v_{TOT} N^{-1} x_{ref}} \quad \text{for } i = 1, \dots, c - r \quad (9)$$

where x_i is the mole fraction of component i , x_{ref} is a column vector of mole fractions for r reference components, v_i is the row vector of stoichiometric coefficients of component i for each of the r reactions, N is an invertible and square matrix formed from the stoichiometric coefficients of the reference components in the r reactions, and v_{TOT} is a row vector where each element corresponds to the sum of stoichiometric coefficients for all components that participate in each of the r reactions, respectively. The transformed mole fractions in reactive systems are similar to the mole fractions in non-reactive mixtures and the sum of all transformed mole fractions must equal unity, or $\sum_{i=1}^{c-r} X_i = 1$, but a transformed mole fraction can be negative or positive depending on the reference components, number and type of reactions. Note that X are related to x using the reaction equilibrium constants $K_{eq,k}$:

$$K_{eq,k} = \prod_{i=1}^c a_i^{v_{ik}} \quad k = 1, \dots, r \quad (10)$$

where v_{ik} is the stoichiometric coefficient of component i in reaction k , and a_i is the activity of component i , respectively. To evaluate thermodynamic properties in reactive systems using this approach, the mole fractions x_i are obtained from the transformation procedure $X \rightarrow x$ using Eqs. (9) and (10). These mole fractions (x) satisfy the stoichiometry requirements and are chemically equilibrated. In this study, the bisection method is used for variable transformation $X \rightarrow x$ in single reactive systems, while the Newton method is applied for multireactive systems. As indicated by Ung and Doherty [47], it is not possible to find multiple solutions for x_{ref} during variable transformation $X \rightarrow x$ because only one solution set of x simultaneously satisfies the chemical equilibrium equations and corresponds to the specified values of the transformed composition variables.

Then, the reactive tangent plane distance function (*RTPDF*) for a c multicomponent and r multireactive system with transformed global composition $Z(Z_1, \dots, Z_{c-r})$ is defined as:

$$RTPDF = \sum_{i=1}^{c-r} Y_i (\mu_{i|Y} - \mu_{i|Z}) \quad (11)$$

where $\mu_{i|Y}$ and $\mu_{i|Z}$ are the chemical potentials of component i calculated at the transformed mole compositions Y and Z , respectively. *RTPDF* represents the displacement from the tangent plane at a composition Z to the transformed molar Gibbs free energy surface at composition Y [12]. The necessary and sufficient condition for global phase stability is given by *RTPDF* ≥ 0 for any transformed composition Y from the whole transformed composition space. Thus, *RTPDF* must be globally optimized with respect to the transformed composition of a trial phase Y for solving the phase stability problem in reacting mixtures.

The global minimization of *TPDF* and *RTPDF* is difficult and requires robust numerical methods since these functions are multivariable, non-convex and highly non-linear. For the case of *TPDF*, several deterministic [9–11,13–19] and stochastic [21,23–25,27,29,31,32,40,42] optimization methods have been reported. On the other hand, few studies have dealt with the global solution of *RTPDF* using a homotopy continuation method [12], simulated annealing [26], differential evolution and tabu search [30]. Note that PSO and its variant have not been applied to solve the phase stability problem of multicomponent reactive and non-reactive mixtures.

The decision variables in phase stability problems are $c - 1$ mole fractions y_i for non-reactive systems and $c - r - 1$ transformed mole fractions Y_i for reactive systems, taking into account that $y_c = 1 - \sum_{i=1}^{c-1} y_i$ and $Y_{c-r} = 1 - \sum_{i=1}^{c-r-1} Y_i$. Following previous studies [24,29,32], the constrained global optimization of *TPDF* or *RTDPF* can be transformed into an unconstrained problem by using new decision variables β_i instead of y_i and Y_i . The decision variables $\beta_i \in (0, 1)$ are related to composition variables y and Y by:

$$n_{iy} = \beta_i z_i n_F \quad i = 1, \dots, c \quad (12)$$

$$\hat{n}_{iY} = \beta_i Z_i \hat{n}_F \quad i = 1, \dots, c - r \quad (13)$$

where

$$y_i = \frac{n_{iy}}{\sum_{j=1}^c n_{jy}} \quad i = 1, \dots, c \quad (14)$$

$$Y_i = \frac{\hat{n}_{iY}}{\sum_{j=1}^{c-r} \hat{n}_{jY}} \quad i = 1, \dots, c - r \quad (15)$$

where $n_F = \sum_{i=1}^c n_{iF}$ and $\hat{n}_F = \sum_{i=1}^{c-r} \hat{n}_{iF}$ are the total amount of conventional and transformed moles in the feed composition used for stability analysis, and n_{iy} and \hat{n}_{iY} are the conventional and transformed mole number of component i in trial phase y and Y , respectively. Note that the transformed mole numbers \hat{n}_i are given as:

$$\hat{n}_i = n_i - v_i N^{-1} n_{ref} \quad i = 1, \dots, c - r \quad (16)$$

where n_i is the number of moles of component i and n_{ref} is a column vector of dimension r of the moles of each of the reference components, respectively. The mole fractions z_i and Z_i are obtained from $z_i = n_{iF}/n_F$ and $Z_i = \hat{n}_{iF}/\hat{n}_F$. Eqs. (12)–(15) have been used for all stability calculations performed in this study. Finally, the calculation of *TPDF* and *RTPDF* is straightforward with almost any thermodynamic model because:

$$\frac{\mu_i - \mu_i^0}{R_g T} = \ln \left(\frac{x_i \hat{\varphi}_i}{\varphi_i} \right) = \ln(x_i \gamma_i) \quad (17)$$

where R_g is the universal gas constant, μ_i^0 is the chemical potential of pure component i , $\hat{\varphi}_i$ is the fugacity coefficient of component i in the mixture, φ_i is the fugacity coefficient of pure component, γ_i is the activity coefficient of component i in the mixture, and x_i is the mole fraction of component i in the mixture.

3.2. Phase split calculations

In phase split problems, the main objectives are to correctly establish the number and types of phases existing at equilibrium as well as the composition and quantity of each phase such that the Gibbs free energy of the system is a minimum [7]. At constant temperature and pressure, a c multicomponent and π multiphase non-reactive system achieves equilibrium when its molar Gibbs free energy of mixing (g) is at the global minimum. The correspond-

ing objective function is given by:

$$g = \sum_{j=1}^{\pi} \sum_{i=1}^c n_{ij} \ln(x_{ij} \gamma_{ij}) = \sum_{j=1}^{\pi} \sum_{i=1}^c n_{ij} \ln \left(\frac{x_{ij} \hat{\varphi}_{ij}}{\varphi_i} \right) \quad (18)$$

where n_{ij} is the mole number of component i in phase j , γ_{ij} is the activity coefficient of component i in phase j , and $\hat{\varphi}_{ij}$ is the fugacity coefficient of component i in phase j , respectively. The Gibbs free energy of mixing (g) is used to avoid the calculation of the pure component free energies, which do not influence equilibrium and stability results [46]. For a non-reactive system, g must be minimized with respect to n_{ij} taking into account the following mass balance constraints:

$$\sum_{j=1}^{\pi} n_{ij} = z_i n_F \quad i = 1, \dots, c \quad (19)$$

$$0 \leq n_{ij} \leq z_i n_F \quad i = 1, \dots, c, \quad j = 1, \dots, \pi \quad (20)$$

where z_i is the mole fraction of component i in the feed. In reactive mixtures, the Gibbs free energy minimization is subject to chemical equilibrium restrictions [7]. However, this difficult thermodynamic problem can be readily solved if the Gibbs energy function is expressed in terms of transformed composition variables (X) [46,47]. For these conditions, minimizing the Gibbs free energy is equivalent to the optimization of transformed Gibbs free energy. Then, the transformed Gibbs free energy of mixing (\hat{g}) for a multiphase reactive system is defined as:

$$\hat{g} = \sum_{j=1}^{\pi} \sum_{i=1}^{c-r} \hat{n}_{ij} \ln(x_{ij} \gamma_{ij}) = \sum_{j=1}^{\pi} \sum_{i=1}^{c-r} \hat{n}_{ij} \ln \left(\frac{x_{ij} \hat{\varphi}_{ij}}{\varphi_i} \right) \quad (21)$$

where \hat{n}_{ij} is the transformed mole number of component i in phase j . Assuming a reactive system where all transformed composition variables are positive, the material balances are described as follows:

$$\sum_{j=1}^{\pi} \hat{n}_{ij} = Z_i \hat{n}_F \quad i = 1, \dots, c - r \quad (22)$$

$$0 \leq \hat{n}_{ij} \leq Z_i \hat{n}_F \quad i = 1, \dots, c - r, \quad j = 1, \dots, \pi \quad (23)$$

where Z_i is the transformed mole fraction of component i in the feed.

For phase equilibrium calculations in non-reactive and reactive systems, g and \hat{g} are the objective functions which, due to the non-linear nature of thermodynamic models, are generally multivariable and non-convex. As indicated, simulated annealing and genetic algorithms [24], tabu search [28], tunneling method [20], differential evolution [29,32] and particle swarm optimization [41,42] have been used for performing Gibbs energy minimization in non-reactive systems. To date, PSO has been applied in binary and ternary systems. In contrast, few stochastic methods have been tested and applied for phase equilibrium calculations in reactive systems, especially using reaction-invariant composition variables [26,30], and preliminary results [43] have suggested that PSO appears to be a robust strategy for the global minimization of \hat{g} . To the best of our knowledge, no one has reported a detailed evaluation and comparison of PSO and its variants for Gibbs energy minimization in both multicomponent reactive and non-reactive systems.

To perform an unconstrained minimization of g and \hat{g} , we can again use a set of new variables instead of n_{ij} and \hat{n}_{ij} as optimization targets. The introduction of these variables eliminates the restrictions imposed by material balances, reduces problem dimensionality, and the optimization problem is transformed to an

unconstrained one [24,29,30,32]. For multiphase non-reactive systems, real variables $\beta_{ij} \in (0, 1)$ are defined and employed as decision variables by using the following expressions:

$$n_{i1} = \beta_{i1} z_i n_F \quad i = 1, \dots, c \quad (24)$$

$$n_{ij} = \beta_{ij} \left(z_i n_F - \sum_{m=1}^{\pi-1} n_{im} \right) \quad i = 1, \dots, c, \quad j = 2, \dots, \pi - 1 \quad (25)$$

$$n_{i\pi} = z_i n_F - \sum_{j=1}^{\pi-1} n_{ij} \quad i = 1, \dots, c \quad (26)$$

while for systems subject to chemical equilibrium, we have

$$\hat{n}_{i1} = \beta_{i1} Z_i \hat{n}_F \quad i = 1, \dots, c - r \quad (27)$$

$$\hat{n}_{ij} = \beta_{ij} \left(Z_i \hat{n}_F - \sum_{m=1}^{\pi-1} \hat{n}_{im} \right) \quad i = 1, \dots, c - r, \quad j = 2, \dots, \pi - 1 \quad (28)$$

$$\hat{n}_{i\pi} = Z_i \hat{n}_F - \sum_{j=1}^{\pi-1} \hat{n}_{ij} \quad i = 1, \dots, c - r \quad (29)$$

Using this formulation, all trial compositions will satisfy the material balances allowing the easy application of optimization strategies [24,29,32]. For Gibbs energy minimization, the number of phases existing at the equilibrium is assumed to be known *a priori* and the number of decision variables is $c \cdot (\pi - 1)$ for non-reactive and $(c - r) \cdot (\pi - 1)$ for reactive systems, respectively.

4. Results and discussion

4.1. Description of phase equilibrium problems

We have tested and compared the performance of PSO and its variants using reactive and non-reactive systems with dimension ranging from 2 to 10. Several systems are multicomponent (i.e., $c \geq 3$) and their thermodynamic properties are represented

with equation of state, solution model and ideality. Our collection of test problems includes systems with vapor–liquid and liquid–liquid equilibrium. A brief description of all examples are given in Tables 2–4 and detailed global solutions of all phase equilibrium problems can be found in Refs. [14,16,24–26,30]. The objective functions (i.e., *TPDF*, *RTPDF*, g and \hat{g}) have at least one local minimum, which corresponds to a trivial solution, for all tested conditions. In addition, the selected conditions involve feed compositions near phase boundaries, which are generally challenging for any algorithm. Most of the selected phase equilibrium problems have been used for testing other deterministic and stochastic optimization strategies, e.g. [9,12,14–16,21,22,24–26,29–31].

4.2. Parameter tuning of PSO-based methods

The key parameters of PSO and its variants have been tuned by finding the global minimum of several phase stability and equilibrium problems. For this purpose, we have considered systems with different degrees of difficulty: example nos. 3 and 5 for non-reactive systems and example nos. 4 and 8 for reactive mixtures. Parameter tuning was performed by varying one parameter at a time while the rest are fixed at nominal values, which were established using values reported in the literature and results of preliminary calculations (not reported in this paper). The tested and suggested parameter values for each PSO-based method are presented in Table 5. For calculations performed in this study, we set $n_p = 10n_{var}$ (i.e., swarm size) and $n_b = 0.25n_p$ (i.e., neighborhood size) in all PSO variants because our preliminary calculations suggest that these parameter values are a reasonable compromise between numerical effort and reliability. All numerical experiments were performed on an Intel Pentium M 1.73 GHz processor with 504 MB of RAM. This computer performs 254 million floating point operations per second (MFlops) for the LINPACK benchmark program (available at <http://www.netlib.org/>) for a matrix of order 500.

4.3. Comparison of PSO and its variants in phase stability and equilibrium calculations

Having performed parameter tuning, we now compare the performance of PSO-based methods. In order to facilitate understanding and to make the performance difference between

Table 2

Examples selected for phase stability and equilibrium calculations in non-reactive systems using particle swarm optimization and its variants.

No.	System	Feed	Thermodynamic models	Reference
1	<i>n</i> -Butyl acetate + water	$z(0.5, 0.5)$ at 298 K and 101.325 kPa	NRTL model. Model parameters reported by Rangaiah [24].	[14,15,24,29,42]
2	Toluene + water + aniline	$z(0.29989, 0.20006, 0.50005)$ at 298 K and 101.325 kPa	NRTL model. Model parameters reported by McDonald and Floudas [14].	[14,24,29,42]
3	$N_2 + C_1 + C_2$	$z(0.3, 0.1, 0.6)$ at 270 K and 7600 kPa	SRK EoS with classical mixing rules. Model parameters reported by Bonilla-Petriciolet et al. [25].	[16,25,31]
4	$C_1 + H_2S$	$z(0.9813, 0.0187)$ at 190 K and 4053 kPa	SRK EoS with classical mixing rules. Model parameters reported by Rangaiah [24].	[4,9,16,21,24,29,31]
5	$H_2O + CO_2 + 2$ -propanol + ethanol	$z(0.99758, 0.00003, 0.00013, 0.00226)$ at 350 K and 2250 kPa	SRK EoS with classical mixing rules. Model parameters reported by Harding and Floudas [16].	[16,25]
6	$C_2 + C_3 + C_4 + C_5 + C_6$	$z(0.401, 0.293, 0.199, 0.0707, 0.0363)$ at 390 K and 5583 kPa	SRK EoS with classical mixing rules. Model parameters reported by Bonilla-Petriciolet et al. [25].	[25]
7	$C_1 + C_2 + C_3 + C_4 + C_5 + C_6 + C_{7-16} + C_{17+}$	$z(0.7212, 0.09205, 0.04455, 0.03123, 0.01273, 0.01361, 0.07215, 0.01248)$ at 353 K and 38500 kPa	SRK EoS with classical mixing rules. Model parameters reported by Harding and Floudas [16].	[16,25]
8	$C_1 + C_2 + C_3 + iC_4 + C_4 + iC_5 + C_5 + C_6 + iC_{15}$	$z(0.614, 0.10259, 0.04985, 0.008989, 0.02116, 0.00722, 0.01187, 0.01435, 0.16998)$ at 314 K and 2010.288 kPa	SRK EoS with classical mixing rules. Model parameters reported by Rangaiah [24].	[22,24,25,29]
9	$C_1 + C_2 + C_3 + C_4 + C_5 + C_6 + C_7 + C_8 + C_9 + C_{10}$	$z(0.6436, 0.0752, 0.0474, 0.0412, 0.0297, 0.0138, 0.0303, 0.0371, 0.0415, 0.0402)$ at 435.35 K and 19150 kPa	SRK EoS with classical mixing rules. Model parameters reported by Bonilla-Petriciolet et al. [25].	[25]

Table 3
Examples selected for phase stability and equilibrium calculations in reactive systems using particle swarm optimization and its variants.

No.	System	Feed and transformed variables	Thermodynamic models	Reference
1	$A_1 + A_2 \leftrightarrow A_3$ $2A_3 \leftrightarrow A_4 + A_2$	Z (0.445, 0.555) at 101.325 kPa and 310 K $X_1 = (x_1 + x_3 + 2x_4)/(1 + x_3 + 2x_4)$ $X_2 = (x_2 + x_3 + x_4)/(1 + x_3 + 2x_4) = 1 - X_1$ Reference components: A_3, A_4	Ideal solution and ideal gas. $K_{eq,1}^1 = \exp(-22.57 + (7368/T))$ $K_{eq,2}^2 = \exp(-7.0265 + (6844.1/T) - (1,391,790/T^2))$ where T is given in K. Model parameters are taken from Bonilla-Petriciolet et al. [26].	[26,47]
2	$A_1 + A_2 \leftrightarrow A_3$, and A_4 as an inert component. (1) Isobutene (2) Methanol (3) Methyl <i>ter</i> -butyl ether (4) n-Butane	Z (0.3, 0.3, 0.4) at 373.15 K and 1013.25 kPa $X_1 = (x_1 + x_3)/(1 + x_3), X_2 = (x_2 + x_3)/(1 + x_3)$ $X_4 = (x_4)/(1 + x_3) = 1 - X_1 - X_2$ Reference component: A_3	Wilson model and ideal gas. $\Delta C_{res}^0/R = -4205.05 + 10.0982T - 0.26677 \ln T$ $\ln K_{eq,1} = (-\Delta C_{res}^0/RT)$, where T is in K. Model parameters are taken from Ung and Doherty [47].	[26,47]
3	$A_1 + A_2 + 2A_3 \leftrightarrow 2A_4$ (1) 2-Methyl-1-butene (2) 2-Methyl-2-butene (3) Methanol (4) <i>Tert</i> -amyl methyl ether	Z (0.354, 0.183, 0.463) at 335 K and 151.9875 kPa $X_1 = (x_1 + 0.5x_4)/(1 + x_4)$ $X_2 = (x_2 + 0.5x_4)/(1 + x_4)$ $X_3 = (x_3 + x_4)/(1 + x_4) = 1 - X_1 - X_2$ Reference component: A_4	Wilson model and ideal gas. $K_{eq,1} = 1.057 \times 10^{-04} e^{4273.5/T}$, where T is in K. Model parameters are taken from Bonilla-Petriciolet et al. [26].	[26]
4	$A_1 + A_2 \leftrightarrow A_3 + A_4$ (1) Acetic Acid (2) n-Butanol (3) Water (4) n-Butyl acetate	Z (0.05, 0.2, 0.75) at 298.15 K and 101.325 kPa $X_1 = x_1 + x_4, X_2 = x_2 + x_4$ $X_3 = x_3 - x_4 = 1 - X_1 - X_2$ Reference component: A_4	UNIQUAC model. $\ln K_{eq,1} = (450/T) + 0.8$, where T is in K. Model parameters are taken from Wasylkiewicz and Ung [12].	[12,26]
5	$A_3 \leftrightarrow A_4$ $A_5 \leftrightarrow A_4$ $A_4 \leftrightarrow A_6$ with A_1 and A_2 inert components.	Z (0.6305, 0.00355, 0.36595) at 101.325 kPa and 333.15 K $X_1 = x_1$ $X_2 = x_2$ $X_6 = x_3 + x_4 + x_5 + x_6 = 1 - X_1 - X_2$ Reference components: A_3, A_4, A_5	Ideal solution and ideal gas. $K_{eq,1} = 1.5$ $K_{eq,2} = 0.15$ $K_{eq,3} = 0.35$ Model parameters are taken from Bonilla-Petriciolet et al. [30].	[30,49]
6	$A_1 + A_2 + 2A_3 \leftrightarrow 2A_4$ with A_5, A_6, A_7 and A_8 as inert components (1) 2-Methyl-1-butene (2) 2-Methyl-2-butene (3) Methanol (4) <i>Tert</i> -amyl methyl ether (5) n-Pentane (6) Isopentane (7) 1-Pentene (8) 2-Pentene	Z (0.16, 0.169, 0.119, 0.02339, 0.213, 0.177, 0.13861) at 310 K and 100 kPa. $X_1 = (x_1 + 0.5x_4)/(1 + x_4)$ $X_2 = (x_2 + 0.5x_4)/(1 + x_4)$ $X_3 = (x_3 + x_4)/(1 + x_4), X_5 = (x_5)/(1 + x_4)$ $X_6 = (x_6)/(1 + x_4), X_7 = (x_7)/(1 + x_4)$ $X_8 = 1 - X_1 - X_2 - X_3 - X_5 - X_6 - X_7$ Reference component: A_4	SRK EoS with conventional mixing rules where all interaction parameters k_{ij} were set to zero. $K_{eq,1} = 1.057 \times 10^{-04} e^{4273.5/T}$, where T is in K. Model parameters are taken from Luyben [50].	[50]
7	$A_1 + A_2 \leftrightarrow A_3$	Z (0.6, 0.4) $X_1 = (x_1 + x_3)/(1 + x_3)$ $X_2 = (x_2 + x_3)/(1 + x_3) = 1 - X_1$ Reference component: A_3	Margules solution model. $(g^E/R_g T) = 3.6x_1x_2 + 2.4x_1x_3 + 2.3x_2x_3$ $K_{eq} = 0.9825$ Model parameters are taken from Bonilla-Petriciolet et al. [26].	[26]
8	$A_1 + A_2 + 2A_3 \leftrightarrow 2A_4$ with A_5 as inert component (1) 2-Methyl-1-butene (2) 2-Methyl-2-butene (3) Methanol (4) <i>Tert</i> -amyl methyl ether (5) n-Pentane	Z (0.1, 0.1, 0.6, 0.2) at 335 K and 151.9875 kPa $X_1 = (x_1 + 0.5x_4)/(1 + x_4)$ $X_2 = (x_2 + 0.5x_4)/(1 + x_4)$ $X_3 = (x_3 + x_4)/(1 + x_4)$ $X_5 = (x_5)/(1 + x_4) = 1 - X_1 - X_2 - X_3$ Reference component: A_4	Wilson model and ideal gas. $K_{eq,1} = 1.057 \times 10^{-04} e^{4273.5/T}$, where T is in K. Model parameters are taken from Bonilla-Petriciolet et al. [26].	[26]
9	$A_1 + A_2 \leftrightarrow A_3$ (1) Propene (2) Water (3) 2-Propanol	Z (0.37, 0.63) at 353.15 K and 100 kPa $X_1 = (x_1 + x_3)/(1 + x_3)$ $X_2 = (x_2 + x_3)/(1 + x_3) = 1 - X_1$ Reference component: A_3	SRK EoS with conventional mixing rules and all interaction parameters equal to zero. $K_{eq} = 23$ Model parameters are taken from Bonilla-Petriciolet et al. [26].	[8,26]

Table 4
Global minimum of selected reactive and non-reactive examples.

No.	Non-reactive			Reactive		
	<i>TPDF</i>	<i>g</i>	Equilibrium	<i>RTPDF</i>	\hat{g}	Equilibrium
1	-0.032466	-0.020198	LLE	-0.019019	-1.298000	VLE
2	-0.294540	-0.352957	LLE	-0.058350	-1.434267	VLE
3	-0.015767	-0.547791	VLE	-0.002058	-1.226367	VLE
4	-0.003932	-0.019892	VLE	-0.065562	-0.301730	LLE
5	-0.012650	-0.0048272	VLE	-0.001591	-1.853908	VLE
6	-0.000002	-1.183653	VLE	-0.113309	-1.798377	VLE
7	-0.002688	-0.838783	VLE	-0.020055	-0.144508	LLE
8	-1.486205	-0.769772	VLE	-0.042742	-1.043199	VLE
9	-0.000020	-1.121176	VLE	-0.024946	-1.347857	VLE

PSO-based methods more explicit, we have employed the performance profile (PP) reported by Dolan and More [48]. PP is an alternative tool for evaluating and comparing the performance of several solvers on a set of test problems. The results of PP allow us to identify the expected performance differences among several solvers and to compare the quality of their solutions by eliminating the bias of failures obtained in a small number of problems. We will give a brief overview of PP, and a detailed description is provided by Dolan and More [48]. Suppose that, for a set of N_{prob} problems (in our case, the collection of phase equilibrium problems reported in Tables 2 and 3) and a set of S solvers (in our case, PSO and its variants tested), we obtain a performance metric $t_{ij} \geq 0$ for every solver $i \in S$ and problem $j \in N_{prob}$. This performance metric should give information on solver reliability, efficiency or another performance measure useful to characterize the capabilities of the solver under evaluation. For each problem $j \in N_{prob}$, we calculate:

$$t_j^* = \min\{t_{ij} | \text{solver } i \in S\} \quad (30)$$

which indicates the best possible performance for problem j among all the solvers tested. For a particular solver i , the set of performance ratios σ_{ij} is determined by:

$$\sigma_{ij} = \frac{t_{ij}}{t_j^*} \quad j \in N_{prob} \quad (31)$$

The performance ratio σ_{ij} of method i for problem j is simply the ratio of the method's performance to the best performance value over all solvers for the same problem. The value of σ_{ij} is 1 for the solver i that performs best on a specific problem j . For every solver $i \in S$, let $\rho_i(\zeta)$ be the fraction of problems for which $\sigma_{ij} \leq \zeta$ where $\zeta \geq 1$. Specifically, we have:

$$\rho_i(\zeta) = \frac{1}{N_{prob}} \text{size}\{j \in N_{prob} : \sigma_{ij} \leq \zeta\} \quad (32)$$

Table 5
Suggested values of parameters in PSO and its variants for phase stability and equilibrium calculations in multicomponent reactive and non-reactive mixtures.

PSO method	Parameter	Tested values	Suggested values
PSO-C	c_1	2.0, 2.5, 2.8, 3.0, 3.5	3.0
	c_2	0.5, 1.0, 1.3, 1.5, 2.0	1.0
PSO-D	$c_{1,0}$	2.0, 2.5, 2.8, 3.5, 3.0	3.0
	l	4.0, 4.1	4.0
PSO-I	c_1	2.0, 2.5, 2.8, 3.0, 3.5	3.5
	c_2	0.5, 1.0, 1.3, 1.5, 2.0	0.5
	w	0.6, 0.8	0.6
PSO-DI	c_1	2.0, 2.5, 2.8, 3.0, 3.5	3.5
	c_2	0.5, 1.0, 1.3, 1.5, 2.0	0.5
	w_0	0.6, 0.8	0.6
PSO-CF	c_1	2.8, 3.0, 3.5	3.5
	l	4.1, 4.5, 5.0	5.0

where the "size" is the number of problems such that the performance ratio σ_{ij} is less than or equal to ζ for solver j . The parameter $\rho_i(\zeta)$ indicates the fraction of problems for which solver i is within a factor of ζ of the best solver (according to the performance metric chosen for solver comparison). Thus, the performance profile of a solver represents the cumulative distribution function of its performance ratios and is a plot of $\rho_i(\zeta)$ versus ζ . Note that $\rho_i(1)$ indicates the probability (i.e., fraction of problems tested) for which solver i was the best solver overall. To identify the best solver using PP, it is only necessary to compare the values of $\rho_i(1)$ for all solvers and to select the highest one.

Our study compares how well the PSO-based methods can estimate the global optimum relative to one another in phase stability and equilibrium calculations. So, we have used the following performance metric for a systematic assessment of PSO reliability:

$$t_{ij} = \hat{f}_{ij}^{calc} - f_j^* \quad (33)$$

where f_j^* is the known global optimum of the objective function for problem j and \hat{f}_{ij}^{calc} is the mean value of the objective function calculated by the stochastic method i over 100 runs performed with random initial values for problem j . This performance metric is useful to identify the algorithm that provides the most accurate value of the global minimum in phase equilibrium problems and we consider that it is suitable for comparison of PSO-based methods. In this study, performance profiles are calculated at different levels of efficiency, which are obtained by varying the stopping conditions $Iter_{max}$ and Sc_{max} , to investigate the behavior of PSO algorithms.

First we assess the effect of stopping criterion $Iter_{max}$ on performance of PSO-based methods. To directly compare the reliability of PSO and its variants, we keep the number of function evaluations (NFE_{stoc}) constant using $Iter_{max}$ alone as stopping condition and evaluate the quality of the results obtained. Note that fair algorithm comparisons can only occur if all solvers have a uniform stopping condition. Fig. 2a shows the results of $\rho_i(1)$ versus $Iter_{max}$ for PSO and its variants in phase stability and equilibrium calculations of both reactive and non-reactive systems using Eq. (33) as performance metric. Our results indicate that PSO-C offers the best performance and shows the highest probability for finding the best solutions in the collection of phase equilibrium problems used in the present study. It is clear from Fig. 2a that the probability $\rho_i(1)$ of PSO-C increases as $Iter_{max}$ increases. In fact, PSO-C dominates the other PSO variants and is the best method throughout the range of $Iter_{max}$ tested. On the other hand, PSO-CF appears to be the second best algorithm for this stopping criterion especially at early iterations. But, its probability $\rho_i(1)$ decreases when $Iter_{max}$ increases. Overall, results of PP indicate that the best solutions found by PSO-D, PSO-I and PSO-DI are worse than the best solution found by PSO-C and PSO-CF in the global optimization of *TPDF*, *RTPDF*, *g* and \hat{g} .

The results of PP using Sc_{max} alone as stopping condition are reported in Fig. 2b. At low values of Sc_{max} , PSO-CF has the high-

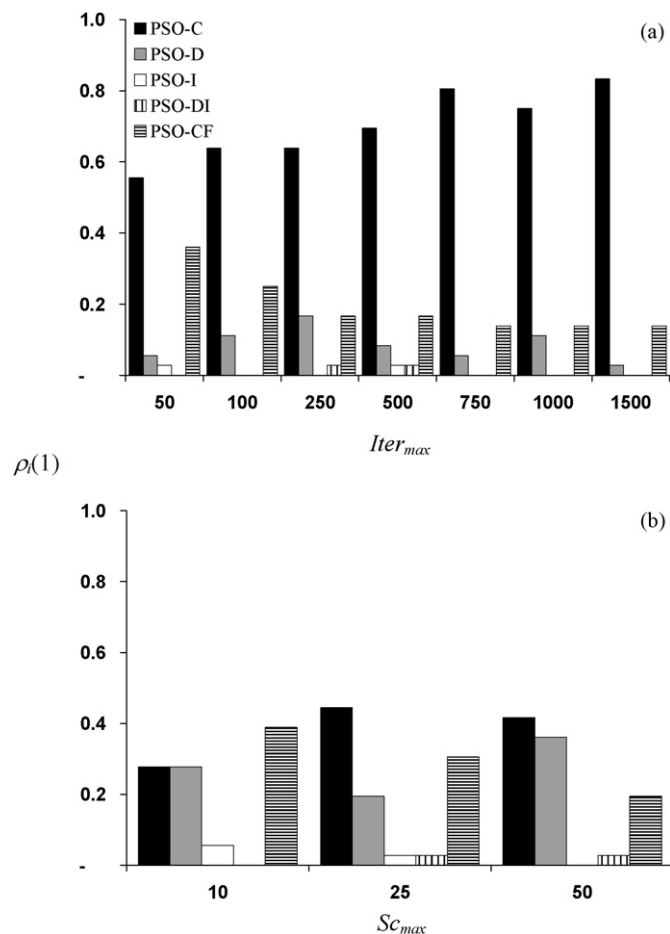


Fig. 2. Results of performance profiles for the comparison of PSO and its variants in phase stability and equilibrium calculations of reactive and non-reactive mixtures. Performance metric: $t_{ij} = \hat{f}_{ij}^{calc} - f_j^*$. Stopping condition of PSO: (a) a maximum number of iterations and (b) a maximum number of successive iterations without improvement in the best function value. Note that missing bars indicate that the probability $\rho_i(1)$ for solver i is 0.0.

est probability $\rho_i(1)$ for finding the best solution in reactive and non-reactive phase stability and equilibrium problems. However, PSO-CF is overtaken by PSO-C and PSO-D at higher values of Sc_{max} . Once more, PSO-I and PSO-DI show the worst performance for finding the global optimum in phase equilibrium problems. It appears that the use of inertia parameter w (with constant and dynamic values) does not significantly improve the reliability of PSO for solving phase stability and equilibrium problems with or without chemical equilibrium. In addition, the linear decrease in inertia term appears to be more competitive than a constant inertia term for solving these thermodynamic problems. Our observations are in agreement with results reported in the literature for benchmark problems [34,35], which indicates that the constriction approach seems superior to the introduction of inertia term. However, our results suggest that this trend depends on the stopping condition used for the PSO algorithm in phase equilibrium problems.

To compare algorithm efficiency, we used NFE_{stoc} as performance metric (i.e., $t_{ij} = NFE_{stoc}$) and the results of PP are given in Fig. 3 employing Sc_{max} alone as stopping condition. Even though PSO-I and PSO-DI showed the worst performance in terms of locating the global optimum, these methods are more efficient than PSO-C and PSO-D. Note that PSO-CF is also more competitive than PSO-C and PSO-D from the standpoint of numerical effort requirements. The percentage reduction in NFE_{stoc} of PSO-DI and PSO-I compared to PSO-C is around 0.4–29.6 and 0.8–29.2%, respectively.

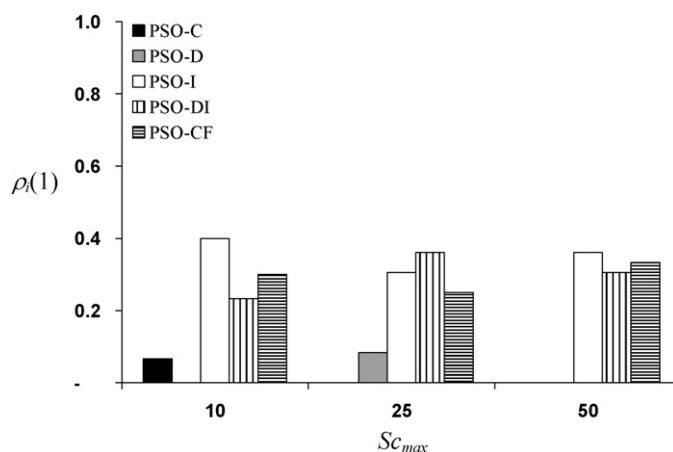


Fig. 3. Results of performance profiles for the comparison of PSO and its variants in phase stability and equilibrium calculations of reactive and non-reactive mixtures. Performance metric $t_{ij} = NFE_{stoc}$ and Sc_{max} as stopping condition of PSO algorithms. Note that missing bars indicate that the probability $\rho_i(1)$ for solver i is 0.0.

As indicated by Ali and Kaelo [35], the usual variants to the original PSO have been proposed to make it faster. Unfortunately, these variants improve the convergence rate of PSO but compromise reliability in reactive and non-reactive phase stability and equilibrium calculations.

In conclusion, the order of reliability of the PSO algorithms in finding the global minimum for phase equilibrium problems is PSO-C > PSO-CF > PSO-D > PSO-DI \cong PSO-I using either $Iter_{max}$ or Sc_{max} as stopping condition. Among the PSO variants tested in this study, PSO-C is the best from the standpoint of algorithm reliability and its selection is therefore clearly justified for solving phase stability and equilibrium problems in reactive and non-reactive systems.

4.4. Numerical study of the best PSO algorithm in combination with a local optimization method

After selecting the best PSO algorithm, we now perform a comparative study using PSO in combination with a local optimization technique for finding the global minimum accurately and efficiently. Specifically, the point identified by the best PSO algorithm is used as initial guess for a local optimization technique. Note that stochastic optimization methods may require a significant computational effort to improve the accuracy of global solution because they explore the search space of decision variables by creating random movements instead of determining a logical optimization trajectory. This convergence behavior is illustrated in Fig. 4 for some reactive and non-reactive phase equilibrium problems. Therefore, the intensification step is needed for rapid convergence and for improving the accuracy of final solutions once the particles of PSO are clustered around the global optimum especially in multicomponent systems. For local optimization, we have applied and compared two strategies, namely: (a) a quasi-Newton (QN) method implemented in the subroutine DBCONF from IMSL library and (b) a Nelder–Mead (NM) simplex method implemented in the subroutine DBCPOL from IMSL library. The former is an efficient gradient-based method that calculates the gradient via finite differences and approximates the Hessian matrix according to the BFGS formula, whereas the latter is a direct search method not requiring derivatives. The default values of both DBCONF and DCPOL parameters in the IMSL library were used in our calculations. The performance of the best PSO with local optimization is studied from the standpoints of reliability and efficiency. All algorithms were run 100 times, with random initial values for decision variables and random number seed, on each of the test problems to

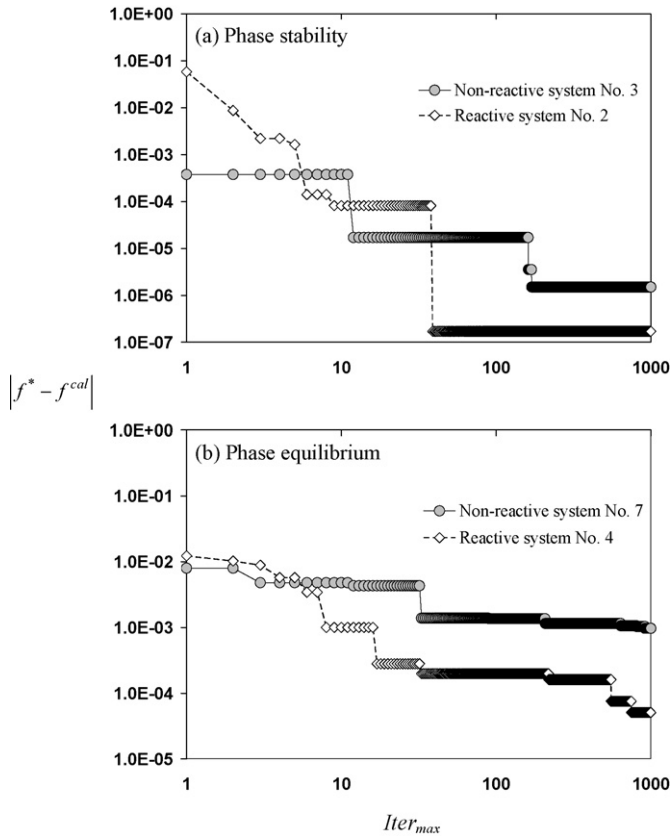


Fig. 4. Convergence histories of the norm $|f^* - f^{cal}|$ of PSO-C in the global minimization of $TPDF$, $RTPDF$, g and \hat{g} for selected reactive and non-reactive examples.

determine the success rate (SR, measured in terms of number of times the algorithm located the global minimum out of 100 trials and reported as percentage) and computational efficiency (measured in terms of average number of function evaluations NFE and CPU time). The average NFE and CPU time were calculated using successful trials only. A trial is considered successful if the global optimum is obtained with an absolute error of 10^{-5} or lower in the objective function value, i.e. $|f^* - f^{cal}| \leq 10^{-5}$. One exception is the non-reactive example no. 5 where an absolute error of 10^{-7} in the objective function g was used to avoid counting local minima as the global optimum. NFE includes both the function calls for evaluating the objective function using the stochastic method (NFE_{stoc}) and the function calls for the local optimization (NFE_{loc}).

The performance of PSO-C implemented with DBCONF and DCPOL subroutines is given in Fig. 5 and Tables 6 and 7. The PSO methods consisting of PSO-C followed by QN or NM are denoted as PSO-CQN and PSO-CNM, respectively. For the sake of brevity, algorithm reliability results are summarized through the global success rate (GSR, %). Specifically, GSR is defined as the total number of successes out of all calculations performed on the collection of phase equilibrium problems tested:

$$GSR = \sum_{i=1}^{nb} \frac{SR_i}{N_{prob}} \quad (34)$$

where SR_i is the success rate in the problem i . Overall, the GSR of PSO-CNM is slightly higher than that obtained for PSO-CQN using $Iter_{max}$ and Sc_{max} . As expected, the GSR of both PSO-CNM and PSO-CQN improves as $Iter_{max}$ or Sc_{max} increases (see Fig. 5). Our results show that there is an improvement in the reliability of both PSO-CQN and PSO-CNM using $Iter_{max}$ compared to that of Sc_{max} . This could be because PSO algorithms require sev-

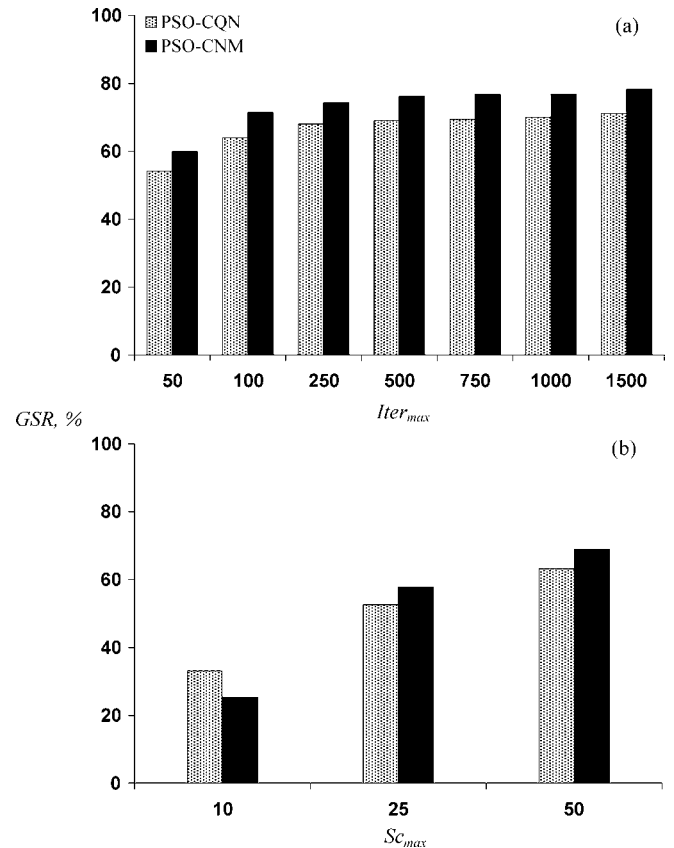


Fig. 5. Global success rate of PSO-CQN and PSO-CNM in phase stability and equilibrium calculations of reactive and non-reactive systems using: (a) $Iter_{max}$ and (b) Sc_{max} as stopping conditions.

eral iterations to improve objective function values after getting stuck at some local optima especially in challenging optimization problems. It is important to note that PSO-CNM offers better performance in reactive phase equilibrium problems than PSO-CQN. This could be because the objective functions $RTPDF$ and \hat{g} appear to be flat near the global solution, affecting the numerical behavior of gradient-based methods. In general, the SR of PSO-CNM is around 100% in the global optimization of $TPDF$ for examples 1–4 and 8 whereas the global optimum of $RTPDF$ is found with a high SR in all reactive examples if proper values of $Iter_{max}$ and Sc_{max} are used. PSO-CNM failed several times to find the global optimum of $TPDF$ in non-reactive example nos. 5–7 and 9. In particular, non-reactive example no. 5 is very challenging and useful for testing new global optimization strategies due to the presence of comparable minima [16]. With respect to phase split calculations, PSO-CNM is also very reliable in the global optimization of g for all non-reactive examples with the exception of example no. 5, where performance is very poor (i.e., 0% SR). For the case of \hat{g} , the reliability of PSO-CNM is close to 100% SR for reactive example nos. 2, 4–8, while this method showed failures in the global optimization of reactive example nos. 1, 3 and 9. On the other hand, PSO-CQN requires a slightly lower NFE than PSO-CNM using $Iter_{max}$ and Sc_{max} (see results reported in Tables 6 and 7). The CPU time ranged from 0.01 to 5.88 s for non-reactive examples and from 0.16 to 101.1 s in reactive examples in all calculations performed using PSO-CNM. Note that the CPU time in reactive systems is higher due to the variable transformation procedure $X \rightarrow x$ involved in the calculation of thermodynamic properties especially when EoS models and high values of $Iter_{max}$ (>1000) are used.

Finally, the performance of PSO-CNM is compared with results reported by Rahman et al. [42] for repulsive particle swarm opti-

Table 6
NFE of PSO-CNM and PSO-CQN in phase stability and equilibrium calculations in selected non-reactive examples.

Example	f	n_{var}	Method	NFE for ^a									Sc_{max}		
				$Iter_{max}$											
				50	100	250	500	750	1000	1500	10	25	50		
1	TPDF	2	PSO-CQN	1029	2,026	5,023	10,019	15,019	20,018	30,018	481	1027	1,958		
			PSO-CNM	1057	2,055	5,052	10,050	15,049	20,048	30,047	536	1030	1,905		
	g	PSO-CQN	1051	2,048	5,045	10,040	15,038	20,037	30,036	553	1248	2,313			
		PSO-CNM	1074	2,073	5,071	10,071	15,070	20,069	30,068	623	1259	2,354			
6	TPDF	5	PSO-CQN	2718	5,219	12,722	25,223	37,722	50,220	75,223	1,915	3013	5,506		
			PSO-CNM	2769	5,281	12,769	25,264	37,758	50,266	75,271	1,830	2972	5,349		
	g	PSO-CQN	2677	5,169	12,666	25,162	37,661	50,162	75,159	1,477	2680	4,680			
		PSO-CNM	2788	5,293	12,787	25,283	37,783	50,285	75,284	1,896	2790	4,850			
7	TPDF	8	PSO-CQN	4652	8,766	20,748	40,771	60,762	80,763	120,757	4,216	5806	9,387		
			PSO-CNM	4573	8,707	20,692	40,724	60,735	80,712	120,678	3,752	5653	9,366		
	g	PSO-CQN	4728	8,718	20,713	40,711	60,712	80,706	120,700	2,411	4371	7,852			
		PSO-CNM	4413	9,114	21,201	41,226	61,186	81,169	121,161	2,559	5932	9,807			
9	TPDF	10	PSO-CQN	5861	10,925	25,959	51,008	76,019	101,044	151,072	5,877	7340	11,420		
			PSO-CNM	5752	10,858	25,908	50,969	75,929	100,922	150,968	4,105	7360	12,024		
	g	PSO-CQN	5858	11,034	26,030	51,028	76,030	101,036	151,029	NC	7121	10,213			
		PSO-CNM	5871	11,124	26,190	51,258	76,298	101,317	151,330	NC	7226	10,237			

^a NC indicates that NFE is not reported because PSO algorithm showed a 0% success rate.

Table 7
NFE of PSO-CNM and PSO-CQN in phase stability and equilibrium calculations in selected reactive examples.

Example	f	n_{var}	Method	NFE for						Sc_{max}			
				$Iter_{max}$									
				50	100	250	500	750	1000	1500	10	25	50
5	RTPDF	3	PSO-CQN	1564	3063	7,562	15,062	22,562	30,063	45,063	744	1625	2909
			PSO-CNM	1611	3109	7,607	15,106	22,605	30,105	45,104	914	1673	2956
	\hat{g}	PSO-CQN	1559	3073	7,586	15,089	22,585	30,083	45,080	681	1471	2928	
		PSO-CNM	1648	3164	7,671	15,174	22,670	30,169	45,165	1008	1558	3017	
6	RTPDF	7	PSO-CQN	3861	7471	17,987	35,542	52,970	70,473	105,546	2162	3761	6834
			PSO-CNM	4020	7518	18,015	35,508	53,005	70,504	105,501	3436	4330	6900
	\hat{g}	PSO-CQN	3849	7414	17,881	35,372	52,832	70,336	105,353	1915	3726	6686	
		PSO-CNM	4091	7623	18,127	35,619	53,123	70,620	105,623	3518	4639	6893	
7	RTPDF	2	PSO-CQN	1053	2051	5,047	10,047	15,046	20,047	30,047	492	1011	1930
			PSO-CNM	1061	2059	5,057	10,056	15,056	20,057	30,057	537	1020	1938
	\hat{g}	PSO-CQN	1070	2070	5,068	10,066	15,064	20,067	30,066	600	1141	2121	
		PSO-CNM	1074	2074	5,072	10,071	15,070	20,070	30,069	648	1140	2124	

mization (RPSO). Rahman et al. [42] studied the performance of RPSO for solving the phase stability and equilibrium problem in the binary system n-butyl acetate and water (example no. 1 from Table 3 of this paper). The stability test of this mixture was successfully performed and RPSO required 25,025 NFE to converge, whereas 7150 NFE were required by RPSO for determining the phase equilibrium compositions. Our results indicate that PSO-CNM can find the global optimum of both TPDF and g with a 100% SR but using a lower NFE than RPSO. Specifically, the NFE of PSO-CNM required to complete the stability test is only 1057 and the phase equilibrium compositions are obtained after 2073 NFE. These results suggest that PSO-CNM is robust and appears to be more efficient than RPSO.

5. Conclusions

This paper reports on a comparative study of particle swarm optimization and several of its variants for performing phase stability and equilibrium calculations in both reactive and non-reactive systems. We have shown and compared the effect that the stopping condition has on the reliability and efficiency of PSO-based methods for solving phase equilibrium problems. Overall, classical particle swarm optimization with constant cognitive and

social parameters offers the best performance from the standpoint of algorithm reliability, whereas the classical variants of particle swarm optimization are effective but not reliable methods to perform the global optimization of TPDF, RTPDF, g and \hat{g} . The results clearly demonstrate that the incorporation of constriction factor or inertia term in the velocity update rule does not provide a significant improvement in PSO performance in terms of the reliability for finding the global optimum. Furthermore, the Nelder–Mead simplex method is more robust than a quasi-Newton method for the intensification step of PSO especially for reactive phase equilibrium calculations. In summary, our results indicate that PSO-CNM is a suitable alternative method for reliably performing phase stability and equilibrium calculations in reactive and non-reactive systems. Further research is underway for development of an efficient and robust hybrid PSO algorithm using other metaheuristics such as simulated annealing or differential evolution.

List of symbols

a_i	activity of component i
c	number of components
c_1	cognitive parameter in PSO
c_2	social parameter in PSO
f	objective function value

g	molar Gibbs free energy of mixing
\hat{g}	transformed molar Gibbs free energy of mixing
G	Gibbs free energy function
$Iter_{max}$	maximum number of iterations for PSO
k	iteration counter
K_{eq}	reaction equilibrium constant
n	mole number
\hat{n}	transformed mole number
n_h	neighborhood size in PSO
n_p	swarm size in PSO
n_{var}	number of optimization variables
N	invertible matrix of stoichiometric coefficients of reference components
N_{prob}	overall number of tested problems
NFE	number of function evaluations
P	pressure
r	number of independent chemical reactions
R_g	universal gas constant
R_1, R_2	random numbers
$RTPDF$	reactive tangent plane distance function
s	position of particles in PSO
SC_{max}	maximum number of successive iterations without improvement in the best function value
SR	success rate of stochastic method
t_{ij}	performance metric of stochastic method
T	temperature
$TPDF$	tangent plane distance function
u	vector of decision variables
ν_i	stoichiometric coefficient of component i
V	velocity of particle in PSO
w	inertia term in PSO
x, y	mole fraction of trial phase
X, Y	transformed mole fraction of trial phase
z	feed mole fraction
Z	transformed feed mole fraction
β_i	decision variable for phase stability and equilibrium calculations
σ	performance ratio
ρ	probability of performance profiles
κ	constriction factor in PSO
μ_i	chemical potential of component i
$\hat{\varphi}_i$	fugacity coefficient of component i in the mixture
φ_i	fugacity coefficient of pure component i
γ_i	activity coefficient of component i in the mixture
π	phase number

Acknowledgement

The authors acknowledge the financial support of CONACYT, Instituto Tecnológico de Aguascalientes and Universidad de Guanajuato.

References

- [1] M. Srinivas, G.P. Rangaiah, *Comp. Chem. Eng.* 30 (2006) 1400–1415.
- [2] J.W. Gibbs, *Trans. Conn. Acad. Arts Sci. II* (1873) 382–404.
- [3] L.E. Baker, A.C. Pierce, K.D. Luks, *Soc. Petrol. Eng. J.* 22 (1982) 731–742.
- [4] M.L. Michelsen, *Fluid Phase Equilib.* 9 (1982) 1–20.
- [5] Y.S. Teh, G.P. Rangaiah, *Chem. Eng. Res. Des.* 80 (2002) 745–759.
- [6] W.D. Seider, S. Widagdo, *Fluid Phase Equilib.* 123 (1996) 283–303.
- [7] W.A. Wakeman, R.P. Stateva, *Rev. Chem. Eng.* 20 (2004) 1–56.
- [8] R.P. Stateva, W.A. Wakeham, *Ind. Eng. Chem. Res.* 36 (1997) 5474–5482.
- [9] A.C. Sun, W.D. Seider, *Fluid Phase Equilib.* 103 (1995) 213–249.
- [10] S.K. Wasykiewicz, L.N. Sridhar, M.F. Doherty, M.F. Malone, *Ind. Eng. Chem. Res.* 35 (1996) 1395–1408.
- [11] F. Jalali, J.D. Seader, *Comp. Chem. Eng.* 23 (1999) 1319–1331.
- [12] S.K. Wasykiewicz, S. Ung, *Fluid Phase Equilib.* 175 (2000) 253–272.
- [13] F. Jalali, J.D. Seader, S. Khaleghi, *Comp. Chem. Eng.* 32 (2008) 2333–2345.
- [14] C.M. McDonald, C.A. Floudas, *AIChE J.* 41 (1995) 1798–1814.
- [15] C.M. McDonald, C.A. Floudas, *Comp. Chem. Eng.* 21 (1997) 1–23.
- [16] S.T. Harding, C.A. Floudas, *AIChE J.* 46 (2000) 1422–1440.
- [17] J.Z. Hua, J.F. Brennecke, M.A. Stadtherr, *Fluid Phase Equilib.* 116 (1996) 52–59.
- [18] S.R. Tessier, J.F. Brennecke, M.A. Stadtherr, *Chem. Eng. Sci.* 55 (2000) 1785–1796.
- [19] G.I. Burgos-Solorzano, J.F. Brennecke, M.A. Stadtherr, *Fluid Phase Equilib.* 219 (2004) 245–255.
- [20] D.V. Nichita, S. Gomez, E. Luna, *Comp. Chem. Eng.* 26 (2002) 1703–1724.
- [21] J. Balogh, T. Csendes, R.P. Stateva, *Fluid Phase Equilib.* 212 (2003) 257–267.
- [22] Y.P. Lee, G.P. Rangaiah, R. Luus, *Comp. Chem. Eng.* 23 (1999) 1183–1191.
- [23] Y. Zhu, H. Wen, Z. Xu, *Chem. Eng. Sci.* 55 (2000) 3451–3459.
- [24] G.P. Rangaiah, *Fluid Phase Equilib.* 187–188 (2001) 83–109.
- [25] A. Bonilla-Petriciolet, R. Vazquez-Roman, G.A. Iglesias-Silva, K.R. Hall, *Ind. Eng. Chem. Res.* 45 (2006) 4764–4772.
- [26] A. Bonilla-Petriciolet, U.I. Bravo-Sanchez, F. Castillo-Borja, S. Frausto-Hernandez, J.G. Segovia-Hernandez, *Chem. Biochem. Eng. Q* 22 (2008) 285–298.
- [27] G. Nagatani, J. Ferrari, L. Cardozo Filho, C.C.R.S. Rossi, R. Guirardello, J. Vladimir Oliveira, M.L. Corazza, Braz. J. Chem. Eng. 25 (2008) 571–583.
- [28] Y.S. Teh, G.P. Rangaiah, *Comp. Chem. Eng.* 27 (2003) 1665–1679.
- [29] M. Srinivas, G.P. Rangaiah, *Comp. Chem. Eng.* 31 (2007) 760–772.
- [30] A. Bonilla-Petriciolet, G.P. Rangaiah, J.G. Segovia-Hernandez, J.E. Jaime Leal, in: G.P. Rangaiah (Ed.), *Stochastic Global Optimization: Techniques and Applications in Chemical Engineering*, World Scientific Inc., in press.
- [31] D.V. Nichita, S. Gomez, E. Luna, *Fluid Phase Equilib.* 194–197 (2002) 411–437.
- [32] M. Srinivas, G.P. Rangaiah, *Ind. Eng. Chem. Res.* 46 (2007) 3410–3421.
- [33] J. Kennedy, R.C. Eberhart, *Proceedings of the IEEE International Conference on Neural Networks*, 2005, pp. 1942–1948.
- [34] J.F. Schutte, A.A. Groenwold, *J. Global Optim.* 31 (2005) 93–108.
- [35] M.M. Ali, P. Kaelo, *Appl. Math. Comput.* 196 (2008) 578–593.
- [36] M. Schwaab, E.C. Biscala Jr., J.L. Monteiro, J.C. Pinto, *Chem. Eng. Sci.* 63 (2008) 1542–1552.
- [37] L. Yiqing, Y. Xigang, L. Yongjian, *Comp. Chem. Eng.* 31 (2007) 153–162.
- [38] F. Herrera, J. Zhang, *Comp. Chem. Eng.* 33 (2004) 1593–1601.
- [39] J.C. Ferrari, G. Nagatani, F.C. Corazza, J.V. Oliveira, M.L. Corazza, *Fluid Phase Equilib.* 280 (2009) 110–119.
- [40] B. Cheng, Q. Zheng, D. Chen, Y. He, *J. Chem. Ind. Eng. (China)* 58 (2007) 2957–2963.
- [41] B. Cheng, D.Z. Chen, *J. Chem. Eng. Chin. Univ.* 22 (2008) 320–324.
- [42] I. Rahman, A.K. Das, R.B. Mankar, B.D. Kulkarni, *Fluid Phase Equilib.* 282 (2009) 65–67.
- [43] A. Bonilla-Petriciolet, J.G. Segovia-Hernández, *Comput. Aided Chem. Eng.* 26 (2009) 635–640.
- [44] Y. Shi, R.C. Eberhart, *Lect. Notes Comp. Sci.* 1447 (1998) 591–600.
- [45] M. Clerc, J. Kennedy, *IEEE Trans. Evol. Comput.* 6 (2002) 58–73.
- [46] S. Ung, M.F. Doherty, *Chem. Eng. Sci.* 50 (1995) 3201–3216.
- [47] S. Ung, M.F. Doherty, *Chem. Eng. Sci.* 50 (1995) 23–48.
- [48] E.D. Dolan, J.J. More, *Math. Program. Ser. A* 91 (2002) 201–213.
- [49] A. Bonilla-Petriciolet, G.A. Iglesias-Silva, K.R. Hall, *Fluid Phase Equilib.* 269 (2008) 48–55.
- [50] W.L. Luyben, *Ind. Eng. Chem. Res.* 44 (2005) 5715–5725.